The regulatory effect of the YY1/miR-HCC2/BAMBI axis on the stemness of liver cancer cells

HUIJIE GAO, HONGXIA FAN and HONG XIE

Department of Pathogen Biology, School of Basic Medical Sciences, Tianjin Medical University, Tianjin, Tianjin 300070, P.R. China

Received October 5, 2022; Accepted February 28, 2023

DOI: 10.3892/ijo.2023.5507

Abstract. Cancer stem cells serve key roles in liver cancer recurrence and metastasis. Therefore, the present study evaluated novel regulators of stem cell factor expression to identify novel therapeutic strategies that could target liver cancer stem cells. Deep sequencing was performed to identify novel microRNAs (miRNAs) that were specifically altered in liver cancer tissues. The expression levels of stem cell markers were investigated by reverse transcription-quantitative PCR and western blotting. Sphere formation assays and flow cytometry were used to assess tumor sphere-forming ability and evaluate the population of cluster of differentiation 90^+ cells. Tumor xenograft analyses were used to evaluate tumorigenicity, metastasis and stemness *in vivo*. Bioinformatics analyses and enhanced green fluorescent protein reporter assays or luciferase reporter assays were performed to identify the direct targets of miR-HCC2 and its upstream transcription factors. MiR-HCC2 strongly promoted the cancer stem cell-like properties of liver cancer cells *in vitro*; it also contributed to tumorigenicity, metastasis and stemness *in vivo*. Bone morphogenic protein and activin membrane-bound inhibitor homolog, a direct target of miR-HCC2, activated the Wnt/β-catenin signaling pathway to promote stemness in liver cancer cells. The transcription factor YY1 bound to the promoter of miR-HCC2 and activated its transcription. The present study demonstrated the importance of miR-HCC2 in the induction of stemness in liver cancer, providing new insights into liver cancer metastasis and recurrence.

Correspondence to: Dr Huijie Gao or Dr Hong Xie, Department of Pathogen Biology, School of Basic Medical Sciences, Tianjin Medical University, 22 Qi Xiang Tai Road, Tianjin, Tianjin 300070, P.R. China
E-mail: gaohuijie@tmu.edu.cn
E-mail: xiehong@tmu.edu.cn

Key words: liver cancer, miR-HCC2, stemness, bone morphogenic protein and activin membrane-bound inhibitor homolog, YY1

Introduction

Liver cancer is among the most common malignancies worldwide; its mortality rate (~8.3%) is high because of its chemotherapy resistance and frequent recurrence (1,2). There is increasing evidence that the onset and progression of liver cancer are driven by a small heterogeneous population of tumor-derived cancer stem cells (CSCs) or tumor-initiating cells (3,4). CSCs in the original tumor have the capacity to self-renew and generate certain differentiated cells; therefore, CSCs have key roles in tumorigenesis, recurrence and metastasis (5-7). Liver CSCs are characterized by the expression of specific cell surface markers, such as cluster of differentiation (CD)13, CD24, CD90, CD133, epithelial cellular adhesion molecule (EpCAM), CD44 and aldehyde dehydrogenase, and stemness-related transcription factors, such as nanog homeobox (Nanog), sex determining region Y-box 2 (Sox2), c-Myc and octamer-binding transcription factor 4 (Oct4) (8-14). However, the molecular mechanisms which underlie the formation of liver CSCs, including the regulation of key genes, have not been elucidated. There is a need for the evaluation of novel regulators of stemness-related factors to identify novel therapeutic strategies that can target liver CSCs. MicroRNAs (miRNAs), a class of small noncoding RNAs, regulate gene expression patterns at the post-transcriptional level; this regulation usually involves binding to the 3'-untranslated region (UTR) of target mRNAs (15). miRNAs have previously been reported to serve important roles in liver cancer (16), particularly in the regulation of stemness in liver cancer cells (17-19). Therefore, liver CSC-specific miRNAs may be useful targets in liver cancer therapy.

Bone morphogenic protein and activin membrane-bound inhibitor (BAMBI) is a transmembrane protein that exhibits high similarity to the extracellular domains of transforming growth factor-β family type I receptors (20,21). BAMBI is regarded as an essential regulator of cell proliferation and differentiation that enhances Wnt/β-catenin signaling in certain cell types (22-25). The activation of Wnt/β-catenin signaling serves an important role in the initial growth and maintenance of CSCs; this process is followed by persistent growth in primary tumor regions, epithelial-to-mesenchymal transition, and CSC re-activation, which leads to tumor growth and metastasis (11,26-28).

Materials and methods

Collection of human liver cancer tissue specimens. A total of 13 liver cancer specimens were obtained from the Cancer Center of Sun Yat-Sen University. All cancers had been confirmed by prior pathological analysis. Written informed consent was obtained from each patient prior to specimen analysis, and ethics approval for the present study was granted by the Ethics Committee of Tianjin Medical University (approval no, TMUhMEC2014004). Information regarding the specimens was presented in Table SI.

Solexa-based deep sequencing and data analysis. Small RNA (<200 bp) was extracted from six liver cancer specimens using the mirVana miRNA isolation kit (cat. no. AM1560; Ambion; Thermo Fisher Scientific, Inc.), according to the manufacturer's protocol. The samples were sent to BGI Genomics (Shenzhen, China) for deep sequencing, and quantified and qualified using an Agilent 2100 Bioanaylzer (Agilent Technologies, Inc.) and a StepOnePlus Real-Time PCR System (Applied Biosystems, Thermo Fisher Scientific, Inc.). A total of 1 μg RNA (≥30 ng/μl) was used to generate a small RNA sequencing library using the TruSeq Small RNA Sample Prep Kit version 2 (cat. no. RS-122-2001 and RS-122-2002; Illumina, Inc.) according to the manufacturer's protocol. The libraries were validated using an Agilent 2100 Bioanalyzer (Agilent Technologies, Inc.) to check the size and purity, and by quantitative PCR using EvaGreen® dye (Jena Bioscience GmbH) to verify the concentration. The loading concentration of the final library was 2 pM. The sequencing to generate single-end reads of 50 bp was performed using an Illumina HiSeq 2000 (Illumina, Inc.) with a TruSeq V3-SBS-HS kit (200 cycles; cat. no. FC-401-3001; Illumina Inc.). Bowtie2 (version 2.2.9; http://bowtie-bio.sourceforge.net/index.shtml), miRBase (version 22; http://mirbase.org/), and miRDeep2 (version 2.0.0.8; https://github.com/rajewsky-lab/mirdeep2) were used to analyze the data (29). Detailed information regarding the specimens was provided in Table SI.

Cell cultures and transfections. Liver cancer HepG2, Hep3B and Huh7 cell lines were purchased from The Cell Bank of Type Culture Collection of the Chinese Academy of Sciences and authenticated by short tandem repeat profiling. Huh7 cells were maintained in Dulbecco's modified Eagle medium (DMEM) (Gibco; Thermo Fisher Scientific, Inc.), and HepG2 and Hep3B cells were maintained in minimum essential medium-α (Gibco; Thermo Fisher Scientific, Inc.) with 10% fetal bovine serum (Gibco; Thermo Fisher Scientific, Inc.), 20 mM 4-(2-hydroxyethyl)-1-piperazineethanesulfonic acid, 100 units/ml penicillin and 100 g/ml streptomycin. The cells were incubated at 37˚C in a humidified atmosphere with 5% CO_2. Lipofectamine™ 2000 reagent (Invitrogen; Thermo Fisher Scientific, Inc.) was used for all transfections in this study, according to the manufacturer's protocol.

Vector construction. Plasmids containing miR-HCC2 or scramble miRNA, which included the precursor sequence of miR-HCC2 or a scramble sequence, were amplified by PCR using Taq DNA polymerase (Invitrogen; Thermo Fisher Scientific, Inc.), and inserted into the pcDNA3 vector (Ambion; Thermo Fisher Scientific, Inc.) between the BamHI and EcoRI sites. Hereafter, the miR-HCC2-overexpressing plasmid and negative scramble miRNA control plasmid are referred to as miR-HCC2 and scramble miRNA. The thermocycling conditions used were as follows: pre-denaturation at 95˚C for 3 min, followed by 32 cycles of denaturation at 94˚C for 30 sec, annealing at 58˚C for 45 sec, elongation at 72˚C for 60 sec, and 72˚C for 5 min at the end to allow complete elongation of all product DNA. The primer sequences were as follows: primary transcript (pri)-miR-HCC2 sense: 5'-CGGGATCCG GGTTTGGATGAGAATAG-3' and antisense: 5'-GGAATT CGCCCCTCTACAGACTCCACC-3; scrambled miRNA sense: TGATTCTAAGTATAGCAGACGTAGGCAGAT GGAGCTT and antisense: AAGCTCCATCTGCCTACG TCTGCTATACTTAGAATCA. To knock down miR-HCC2, 2'-O-methyl-modified antisense oligonucleotides specific for miR-HCC2 [antisense oligonucleotide (ASO)-miR-HCC2] were synthesized, as well as scramble control oligonucleotides (ASO-NC), which were purchased from Shanghai GenePharma Co., Ltd.

The wild-type 3'UTR of BAMBI containing the target sites of miR-HCC2 or its mutant were constructed by annealing the oligos for 5 min at 95˚C and 1 h at room temperature, and cloning them into the pcDNA3-EGFP vector (Tianjin Saier Biotechnology Co., Ltd.) between the BamHI and EcoRI sites.

Total RNA was extracted from Huh7 cells using TRIzol reagent (Invitrogen, Thermo Fisher Scientific, Inc.), according to the manufacturer's protocols. RNA (2 μg) was reverse transcribed into complementary DNA (cDNA) using RevertAid RT Reverse Transcription Kit (cat. no. K1691; Thermo Fisher Scientific, Inc.), according to the manufacturer's protocols. To construct the overexpression vectors for BAMBI and YY1, their respective coding sequences were amplified by PCR from cDNA of Huh7 cells, and inserted into the pcDNA3 vector between the BamHI and XhoI sites. For silencing (shR) vector construction, the synthesized oligonucleotides were annealed and ligated them into the pSilencer2.1/neo vector (Ambion; Thermo Fisher Scientific, Inc.) between the BamHI and HindIII sites.

To generate miR-HCC2 promoter reporter constructs, the respective miR-HCC2-promoter1, miR-HCC2-promoter2 and miR-HCC2-promoter3 sequences from the genomic DNA of Huh7 cells were amplified, and the products were then inserted between the KpnI and BglII sites of the pGL3-Basic vector (Promega Corporation). Fragments with mutated YY1 binding sites in the miR-HCC2 promoter (miR-HCC2 promoter2-mut1 and miR-HCC2 promotor2-mut2) were cloned into the pGL3-Basic vector. All constructs were confirmed using Sanger sequencing by Genewiz, Inc. The primers and oligonucleotides were synthesized by the General Biology Anhui, Co., Ltd. and their sequences were presented in Tables SII and SIII.

Establishment of stably transfected cell lines. 1x10^6 Huh7 and Hep3B cells were transfected with 4 μg of control vector or plasmid expressing miR-HCC2 and incubated for 48 h at 37˚C, then selected using 800 μg/ml G418 and 2 mM/l glutamine for 4 weeks. Subsequently, they were maintained using 200 μg/ml G418 and 2 mM/l glutamine. All cultures were incubated at 37˚C in a humidified atmosphere with 5% CO_2.

RNA extraction and reverse transcription-quantitative PCR (RT-qPCR). Total RNA was extracted from tissue samples and cells using TRIzol reagent (Invitrogen, Thermo Fisher Scientific, Inc.), according to the manufacturer's protocols. RNA (2 μg) was reverse transcribed into complementary DNA using Moloney Murine Leukemia Virus (M-MLV) reverse transcriptase (Promega Corporation) for 60 min at 42˚C, 15 min at 70˚C and then on ice. The subsequent qPCR amplification was performed using a SYBR Premix Ex Taq™ Kit (Promega Corporation) as follows: 95˚C for 3 min, followed by 40 cycles of denaturation at 95˚C for 10 sec, annealing at 60˚C for 30 sec and extension at 72˚C for 30 sec. U6 small nuclear RNA and β-actin were used as internal controls. Relative mRNA expression was calculated using the $2^{-\Delta\Delta Cq}$ method (30). Detailed sequences of all primers were presented in Table SIII.

Enhanced green fluorescent protein (EGFP) reporter assay. To validate the targeting of the 3' UTR of BAMBI by miR-HCC2, pcDNA3 (400 ng), pri-miR-HCC2 (400 ng), ASO-NC (10 pmol) or ASO-miR-HCC2 (10 pmol) was co-transfected with BAMBI-3'UTR (200 ng) or BAMBI-3'UTR-mut (200 ng) in 48-well plates using Lipofectamine™ 2000 (Invitrogen; Thermo Fisher Scientific, Inc.), according to the manufacturer's protocol. The transfected cells were then incubated at 37˚C for 48 h in a humidified atmosphere with 5% CO_2. The red fluorescent protein (RFP) expression vector pDsRed2-N1 (20ng; Takara Bio USA, Inc.) was co-transfected for normalization. At 48 h after transfection, the fluorescence intensities of EGFP and RFP were measured with an F-4500 fluorescence spectrophotometer (Hitachi, Ltd.).

Luciferase reporter assays. Bioinformatics analyses were used to predict the miR-HCC2 promoter using Promoter 2.0 (version 2.0; Department of Health Technology, Technical University of Denmark) and the potential transcription factor binding sites using hTFtarget (http://bioinfo.life.hust.edu.cn/hTFtarget#!/). Cells were then seeded into 48-well plates and transfected with miR-HCC2 promoter reporter vectors with/without mutated YY1 binding sites using Lipofectamine 2000 Reagent (Invitrogen, Thermo Fisher Scientific, Inc.) according to the manufacturer's protocol. Luciferase activities were measured at 48 h post-transfection using the Dual-Luciferase Assay Kit (cat. no. E1910, Promega Corporation), according to the manufacturer's protocols. Firefly luciferase activity was normalized to *Renilla* luciferase activity in each well. The pGL3-Basic vector was used as a negative control. The pGL3-control vector (positive control) contained SV40 promoter and enhancer sequences which have been reported to result in strong expression of luc+ in many types of mammalian cells, and served as a positive control in the dual-luciferase assay (Promega Corporation) (31).

Western blotting. Cellular proteins were extracted using radioimmunoprecipitation assay lysis buffer (Beijing Solarbio Science & Technology Co., Ltd.), and protein concentrations were quantified using a BCA protein assay kit (cat. no. P0010S; Beyotime Institute of Biotechnology) according to the manufacturer's protocols. Equal amounts (10 μg/lane) of protein samples were separated using 8% or 10% SDS-PAGE and transferred onto polyvinylidene fluoride membranes. Membranes were blocked with 5% non-fat milk for 1 h at room temperature and incubated at 4˚C with primary antibodies overnight as follows: BAMBI (1:500; cat. no. SRP07313; Tianjin Saier Biotechnology Co., Ltd.), CD90 (1:500; cat. no. SRP06267; Tianjin Saier Biotechnology Co., Ltd.), Oct4 (1:500; cat. no. SRP05560; Tianjin Saier Biotechnology Co., Ltd.), β-catenin (1:500; cat. no. SRP00118; Tianjin Saier Biotechnology Co., Ltd.), YY1 (1:200; cat. no. SRP01281; Tianjin Saier Biotechnology Co., Ltd.), GAPDH (1:2,000; cat. no. SRP00849; Saier Biotech Co.), Nanog (1:1,000; cat. no. WL03273; Wanleibio Co., Ltd.), Sox2 (1:1,000; cat. no. WL03767; Wanleibio Co., Ltd.), EpCAM (1:1,000; cat. no. R24219; Chengdu Zhengneng Biotechnology Co., Ltd.) and centromere protein A (CENP-A) (1:1,000; cat. no. R22598 Chengdu Zhengneng Biotechnology Co., Ltd.). The membranes were washed three times using TBST (0.05% Tween-20), and incubated with horseradish peroxidase (HRP)-conjugated secondary antibodies (1:2,000; cat. no. SE134; Beijing Solarbio Science & Technology Co., Ltd.) for 1 h at room temperature and visualized using a Pierce ECL Western Blotting kit (Pierce; Thermo Fisher Scientific, Inc.). The protein band images were quantified with ImageJ (version 1.48; National Institutes of Health). GAPDH was used as an endogenous control for normalization of the expression levels of target proteins.

Cell fractionation assay. The cell fractionation assay was conducted using an NE-PER™ Nuclear and Cytoplasmic Extraction kit (cat. no. 78833; Thermo Fisher Scientific, Inc.) according to the manufacturer's protocol. Briefly, Huh7 and HepG2 cells were harvested and washed with phosphate-buffered saline, then incubated with ice-cold CER I reagent for 15 min at 4˚C. Subsequently, CER II extraction reagent was added to the reaction mixture for another 1 min; lysates were then centrifuged at 16,000 x g for 5 min at 4˚C. Each supernatant (cytoplasmic extract) was carefully transferred to a fresh microcentrifuge tube and stored on ice. Each pellet was resuspended in NER extraction reagent and incubated for 40 min on ice; the resulting suspension was centrifuged at 16,000 x g for 10 min at 4˚C, and the supernatant (nuclear extract) was transferred to a fresh microcentrifuge tube and stored on ice. All extracts were analyzed using western blotting.

Sphere formation assay. Single cells (5,000 cells/well) were seeded in triplicate onto ultra-low attachment six-well plates (Corning, Inc.) in DMEM/F12 serum-free medium (Invitrogen; Thermo Fisher Scientific, Inc.) containing 1% penicillin/streptomycin, 20 ng/ml epithelial growth factor (Invitrogen; Thermo Fisher Scientific, Inc.) and 10 ng/ml fibroblast growth factor-2 (Invitrogen; Thermo Fisher Scientific, Inc.). After 10 days incubation at 37˚C, the spheres were imaged and the numbers of spheres formed (diameter >100 μm) was counted manually using an inverted light microscope (Olympus Corporation).

Flow cytometry analysis. Cells were incubated in phosphate-buffered saline (PBS) containing 2% fetal bovine serum (Gibco; Thermo Fisher Scientific, Inc.) at 37˚C for 30 min, then incubated with fluorescein isothiocyanate-conjugated CD90 antibody (1 μg/test; cat. no. FC01818; Boster Biological Technology) at room temperature in the dark for 30 min.

Mouse IgG1 kappa Isotype Control (P3.6.2.8.1) (1 μg/test; cat. no. 11-4714-42; Thermo Fisher Scientific, Inc.) served as the control. Samples were analyzed using a BD FACS Calibur flow cytometer (BD Biosciences), and the results were analyzed using FlowJo 7.6 (FlowJo LLC).

In vivo tumor xenograft analysis. A total of $1x10^6$ Huh7 or Hep3B cells that had been stably transfected with miR-HCC2, control vector or scramble miRNA were suspended in 100 μl serum-free DMEM culture medium and subcutaneously injected into the flanks of six 6-week-old female BALB/c nude mice (Beijing Vital River Laboratory Animal Technology Co., Ltd.; Charles River Laboratories, Inc.) with an average weight of 18 g. Mice were kept under standard laboratory conditions (temperature 22±2˚C; relative humidity 50±10%; 12-h light/dark cycle) with access to food and water *ad libitum*. The health and behavior of mice were monitored every day. The volume of each tumor was assessed on once in the first week and then twice a week as follows: Length x width^2 x 1/2. At, 49 days after implantation, mice were sacrificed by cervical dislocation and the tumors were collected. The weight of each tumor was recorded after the tumor had been collected. Furthermore, 1 x 10^5 Huh7 cells that had been stably transfected with miR-HCC2 or control vector were suspended in 100 μl phosphate-buffered saline and injected into the tail veins of six 5-week-old female BALB/c nude mice with an average weight of 16 g (Beijing Vital River Laboratory Animal Technology Co., Ltd.; Charles River Laboratories, Inc.). The mice were kept under standard laboratory conditions (temperature 22±2˚C; relative humidity 50±10%; 12-h light/dark cycle) with access to food and water *ad libitum*. The health and behavior of mice were monitored every day. At, 11 weeks after injection, mice were sacrificed by cervical dislocation and their lungs and livers were collected. The tumors and tissues were fixed with 10% formalin at room temperature for 72 h and embedded in paraffin. Sections (4 μm) were stained with hematoxylin for 5 min and eosin for 2 min at room temperature for histological examinations and morphometric analysis. Tumor anatomy and pathology were assessed to determine primary tumor growth and metastatic lesion formation. Microscopic tumor nodules were counted in histological sections of mouse lungs and livers under a light microscope (10x magnification; Olympus Corporation). The protein expression levels of Sox2, a stem cell marker, were evaluated using immunohistochemical staining. The paraffin embedded sections were first deparaffinized and heated in citrate buffer for antigen retrieval in boiling bath for 15 min and cooled to room temperature for 30 min, then incubated with 3% hydrogen peroxide in PBS at 37˚C for 5 min and blocked with 3% bovine serum albumin in PBS at 37˚C for 1 h. Slides were incubated overnight at 4˚C with primary antibodies against Sox2 (1:200; cat. no. WL03767; Wanleibio Co., Ltd.), followed by incubation with biotinylated secondary antibodies (1:500; cat. no. ab207995; Abcam) for 1 h at room temperature. Images of the sections were captured under a light microscope (40x magnification; Olympus Corporation) and analyzed using Caseviewer 2.4 (3DHISTECH, Ltd.). Symptoms, including loss of appetite, ≥20% body weight loss, weakness, pain, breathing difficulties or tumor volume reaching 2,000 mm^3 were set as humane endpoints for the present study. However, no mice were sacrificed before the end of tumor xenograft experiments due to display of any of these symptoms. All studies were performed with approval from the Animal Ethics Committee of Tianjin Medical University (approval no. TMULA-201954).

Statistical analysis. GraphPad Prism 5 (GraphPad Software; Dotmatics) was used for statistical analysis. Each experiment was repeated in triplicate. All values were presented as mean ± standard deviation. Differences between two groups were evaluated using two-tailed Student's t-test. Statistical significance among three or more groups was assessed using one way ANOVA followed by Tukey's post hoc test. Gene expression relationships were assessed using Pearson correlation coefficients. $P<0.05$ was considered to indicate a statistically significant difference.

Results

The identification of miR-HCC2 in liver cancer tissues. For the identification of miRNAs associated with liver cancer, deep sequencing was used to profile miRNAs isolated from six liver cancer tissue samples (Table SI). In total, 949 miRNAs were isolated, including five novel miRNAs (Fig. 1A). In the present study, miR-HCC2 was focused on, which demonstrated the second high abundance among the novel miRNAs in liver cancer tissues with the sequence 'UCUGUUUGU CGUAGGCAGAUGG' and was located in *Homo sapiens* chromosome 5, GRCh38.p12 Primary Assembly (National Center for Biotechnology Information Reference Sequence, NC_000005) (32). The other miRNA candidates were assessed in ongoing research by other group members. To confirm the results of deep sequencing, RT-qPCR was used to quantify the RNA expression levels of miR-HCC2 in liver cancer tissues and adjacent non-tumor tissues, and the RNA expression levels of miR-HCC2 were significantly higher in liver cancer tissues than in adjacent non-tumor tissues (Fig. 1B). These results were consistent with the deep-sequencing data and indicated that the expression of miR-HCC2 was upregulated in liver cancer tissues.

MiR-HCC2 participates in the regulation of stem cell-like properties of human liver cancer cells. To evaluate whether miR-HCC2 was associated with stem cell-like properties in human liver cancer cells, HepG2 and Huh7 cells were transfected with miR-HCC2 or ASO-miR-HCC2 and their respective control vectors. After the efficiencies of miR-HCC2 vectors and ASO-miR-HCC2 oligomers had been assessed (Fig. 1C), the protein expression levels of a cell surface marker (CD90) and four stem cell markers (Oct4, Nanog, Sox2, and EpCAM) were evaluated. As shown in Fig. 1C and D, the overexpression of miR-HCC2 significantly increased the mRNA and protein expression levels of the surface marker CD90 and the stem cell markers in transiently transfected HepG2 and Huh7 cells; furthermore, the inhibition of miR-HCC2 significantly decreased the mRNA and protein expression levels of these markers. Stable miR-HCC2-overexpressing Huh7 cells demonstrated significantly higher protein and mRNA expression levels of the stem cell markers, compared with the control cells (Fig. 1E). Sphere formation assays demonstrated significantly higher numbers of spheres (≥100 μm)

A

Name	Reads in HBV+ sample	Reads in HBV- sample	Fold change	P-value
miR-HCC1	1183	406	Log_2 1.47744396	1.0353×10^{-80}
miR-HCC2	85	20	Log_2 2.02203575	2.7297×10^{-10}
miR-HCC3	52	7	Log_2 2.82776498	2.1590×10^{-9}
miR-HCC4	36	17	Log_2 1.96692641	0.0145
miR-HCC5	45	11	Log_2 1.01699519	7.3156×10^{-6}

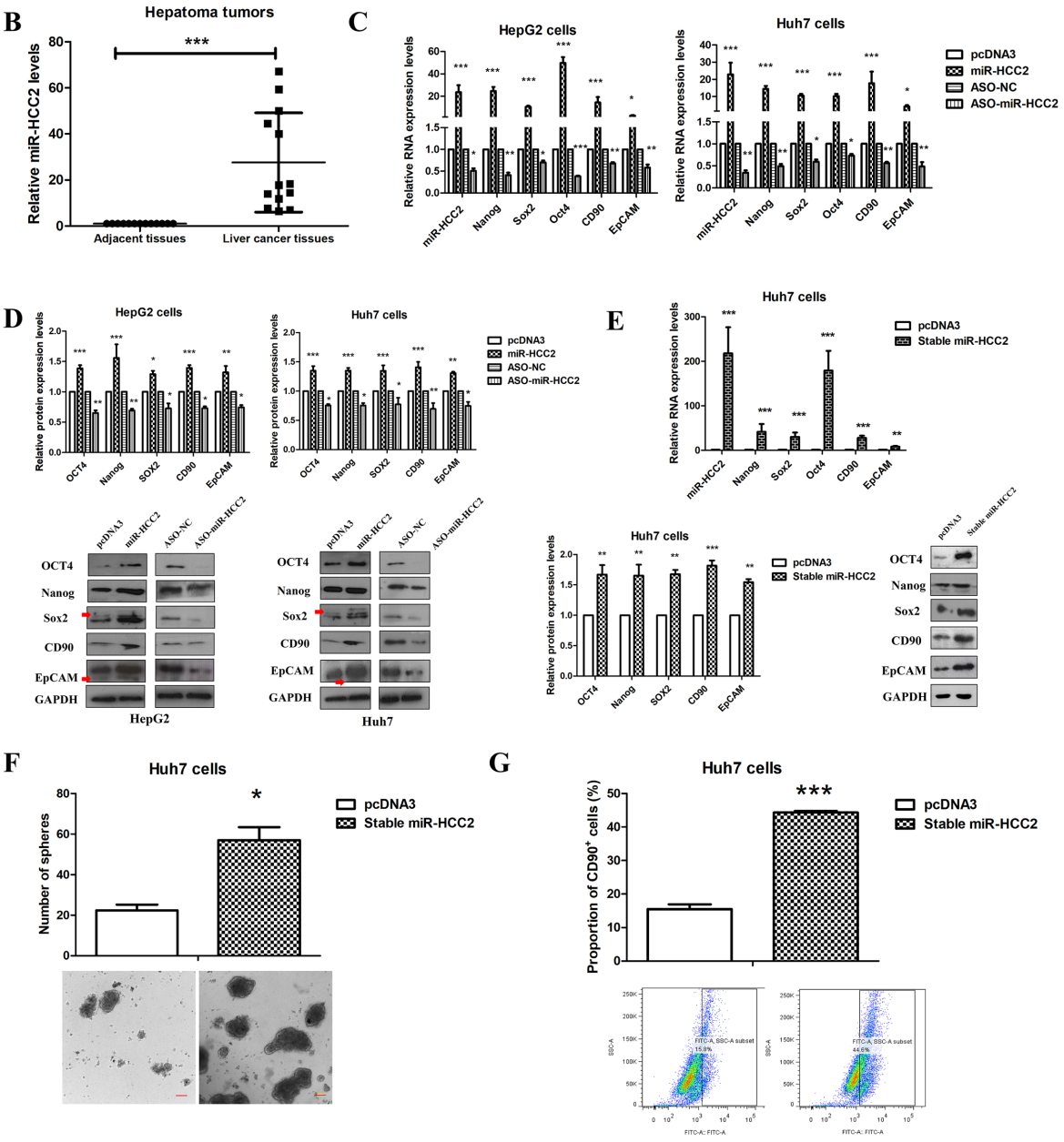

Figure 1. MiR-HCC2 is upregulated in liver cancer tissues and promotes stem cell-like properties in human liver cancer cells. (A) Sequencing reads and statistics of five representative miRNAs identified by deep sequencing. (B) Relative levels of miR-HCC2 in liver cancer tissues and adjacent non-tumor tissues (n=13). U6 RNA was used for normalization. Relative (C) mRNA and (D) protein expression levels of stemness markers in transiently transfected HepG2 and Huh7 cells were assessed by RT-qPCR and western blotting assays, respectively. The arrows indicated nonspecific bands. (E) The mRNA and protein expression levels of miR-HCC2 and stemness markers in stable miR-HCC2-overexpressing Huh7 cells. The samples were derived from the same experiment and the blots were processed in parallel. (F) Tumor sphere-formation assays indicated an enhanced sphere formation ability in stable miR-HCC2-overexpressing Huh7 cells. Scale bar=100 μm. (G) Evaluation of the proportion of $CD90^+$ cells among transfected Huh7 cells. All experiments were performed at least in triplicate. Data are presented as mean ± standard deviation. *P<0.05, **P<0.01 and ***P<0.001 compared with the corresponding control group (miR-HCC2 vs. pcDNA3, ASO-miR-HCC2 vs. ASO-NC and stable miR-HCC2 vs. pcDNA3). miR, microRNA; Nanog, nanog homeobox; Sox2, sex determining region Y-box 2; Oct4, octamer-binding transcription factor 4; CD90, cluster of differentiation 90; EpCAM, epithelial cellular adhesion molecule; ASO, antisense oligonucleotide; NC, negative control.

in stable miR-HCC2-overexpressing Huh7 cells compared with the control cells (57 vs. 22, Fig. 1F), which suggested that miR-HCC2 dramatically enhanced the sphere formation capacities of Huh7 cells. Moreover, flow cytometry analysis was performed to assess the proportion of $CD90^+$ cells in stable miR-HCC2-overexpressing cell lines. The proportion of $CD90^+$ cells was significantly greater among stable miR-HCC2-overexpressing Huh7 cells (mean, 44.3 vs. 15.5%), compared with the control cells (Fig. 1G).

Collectively, these results demonstrated that miR-HCC2 promoted stem cell-like properties in human liver cancer cells by increasing sphere formation, enhancing the proportion of $CD90^+$ cells, and increasing mRNA and protein expression levels of stemness-related genes.

MiR-HCC2 enhances the tumorigenicity, metastasis and stemness of liver cancer cells in nude mice. To evaluate the effects of miR-HCC2 on tumorigenicity and tumor metastasis *in vivo*, subcutaneous and intravenous injections of stable miR-HCC2-overexpressing Huh7 or Hep3B cells into nude mice were performed. A nude mouse xenograft-formation assay was used to evaluate the effects of miR-HCC2 overexpression on the tumorigenicity of liver cancer cells. The mean tumor weight and mean tumor volume (Fig. 2A-C) were significantly greater in the miR-HCC2 group than in the control group. The RNA expression levels of miR-HCC2 and stemness-related markers in mouse tumors derived from stable miR-HCC2-overexpressing Huh7 or Hep3B cells were significantly greater than those in mouse tumors derived from the corresponding control cells (Fig. 2D). MiR-HCC2-overexpressing tumors exhibited poorly differentiated carcinoma morphology and increased cell mitosis, whereas control tumors exhibited highly differentiated carcinoma morphology with low malignancy (upper panel in Fig. 2E and upper panel in Fig. S1). Considering that α-fetoprotein (AFP), a marker for liver cell injury, has important roles in tumor growth and carcinogenesis (33), the expression of AFP was evaluated in mouse tumors. AFP mRNA expression levels were significantly higher in miR-HCC2-overexpressing tumors than in the control tumors (Fig. 2D). Furthermore, immunohistochemical analysis of Sox2 protein expression patterns demonstrated that miR-HCC2-overexpressing cells exhibited markedly higher Sox2 protein expression levels in xenografts, compared with control cells (lower panel in Fig. 2E and Fig. S1), which indicated that miR-HCC2 overexpression promoted cell growth and stemness.

Stable miR-HCC2-overexpressing Huh7 cells were intravenously injected into nude mice via the tail vein to assess the effects of miR-HCC2 on tumor metastasis. The injection of Huh7 cells overexpressing miR-HCC2 led to significantly increased tumor incidence *in vivo*, compared with the injection of Huh7 cells containing the control vector. Two of six (2/6) mice injected with stable miR-HCC2-overexpressing Huh7 cells developed lung and liver metastases, whereas no mice in the control group developed lung or liver metastases (Fig. 2F). Multiple tumor nodules were evident in the lungs and livers of the stable miR-HCC2-overexpressing group, whereas no tumor nodules were visible in the control group. Similarly, hematoxylin and eosin staining demonstrated poorly differentiated carcinoma morphology and increased cell mitosis in lung and liver metastases caused by miR-HCC2-overexpressing Huh7 cells. Immunohistochemistry demonstrated that Sox2 protein expression was markedly increased in both types of metastases with miR-HCC2 overexpression, compared with the control groups (Fig. 2G). The RNA expression levels of miR-HCC2 and the stem cell markers were significantly increased by the injection of stable miR-HCC2-overexpressing Huh7 cells, compared with the control group (Fig. 2H).

These results suggested that miR-HCC2 enhanced the tumorigenicity, metastasis and stemness of liver cancer cells *in vivo*.

BAMBI contributes to stem cell-like properties in human liver cancer cells. miRNAs reportedly target multiple host genes to exert their functions (34). Previous studies have reported that BAMBI was a direct target of miR-HCC2 and a marker of liver CSCs (32,35). BAMBI contributes to enhanced Wnt/β-catenin signaling, which is involved in the regulation of the initial growth and maintenance of CSCs (24,26-28). In the present study, the direct interaction between miR-HCC2 and BAMBI was assessed using an enhanced green fluorescent protein (EGFP) reporter system; the results demonstrated that miR-HCC2 could directly target and upregulate BAMBI expression (Fig. S2). To further assess the role of BAMBI in the regulation of the stemness of human liver cancer cells, overexpression and shR vectors were constructed and then transfected into HepG2 and Huh7 cells. The overexpression or inhibition of BAMBI, respectively, significantly enhanced or reduced the stemness-related gene mRNA and protein expression levels, sphere formation and the proportion of $CD90^+$ cells (Fig. 3A-F). These results indicated that BAMBI contributed to the stem cell-like properties of human liver cancer cells.

Knockdown of BAMBI abolishes miR-HCC2-related effects on stem cell-like properties in human liver cancer cells. BAMBI and miR-HCC2 demonstrated similar effects on stem cell-like properties in liver cancer cells and the expression of BAMBI was positively regulated by miR-HCC2; therefore, whether the effects of miR-HCC2 on stemness in liver cancer cells were mediated by the upregulation of BAMBI expression was evaluated. When the plasmids miR-HCC2 and shR-BAMBI were co-transfected into liver cancer cells, the miR-HCC2-mediated increases in the stemness-related gene mRNA and protein expression levels, sphere formation and the proportion of $CD90^+$ cells were markedly abrogated by BAMBI inhibition (Fig. 4A-F). Overall, the knockdown of BAMBI abolished the stem cell-like properties elicited by miR-HCC2, which demonstrated that BAMBI was a direct functional target of miR-HCC2 in terms of the induction of stemness in liver cancer cells.

BAMBI activates Wnt/β-catenin signaling, which promotes stemness in liver cancer cells. It has been previously reported that BAMBI exerts its functions through the Wnt/β-catenin signaling pathway (22,23). The Wnt/β-catenin signaling pathway is important in cancer, stem cell control and CSC biology (35-37). To elucidate the mechanism by which BAMBI contributes to stemness in liver cancer cells, the present study assessed whether the expression levels of β-catenin and the transcription of Axin2 were affected by BAMBI in liver cancer cells. RT-qPCR and western blotting analyses demonstrated

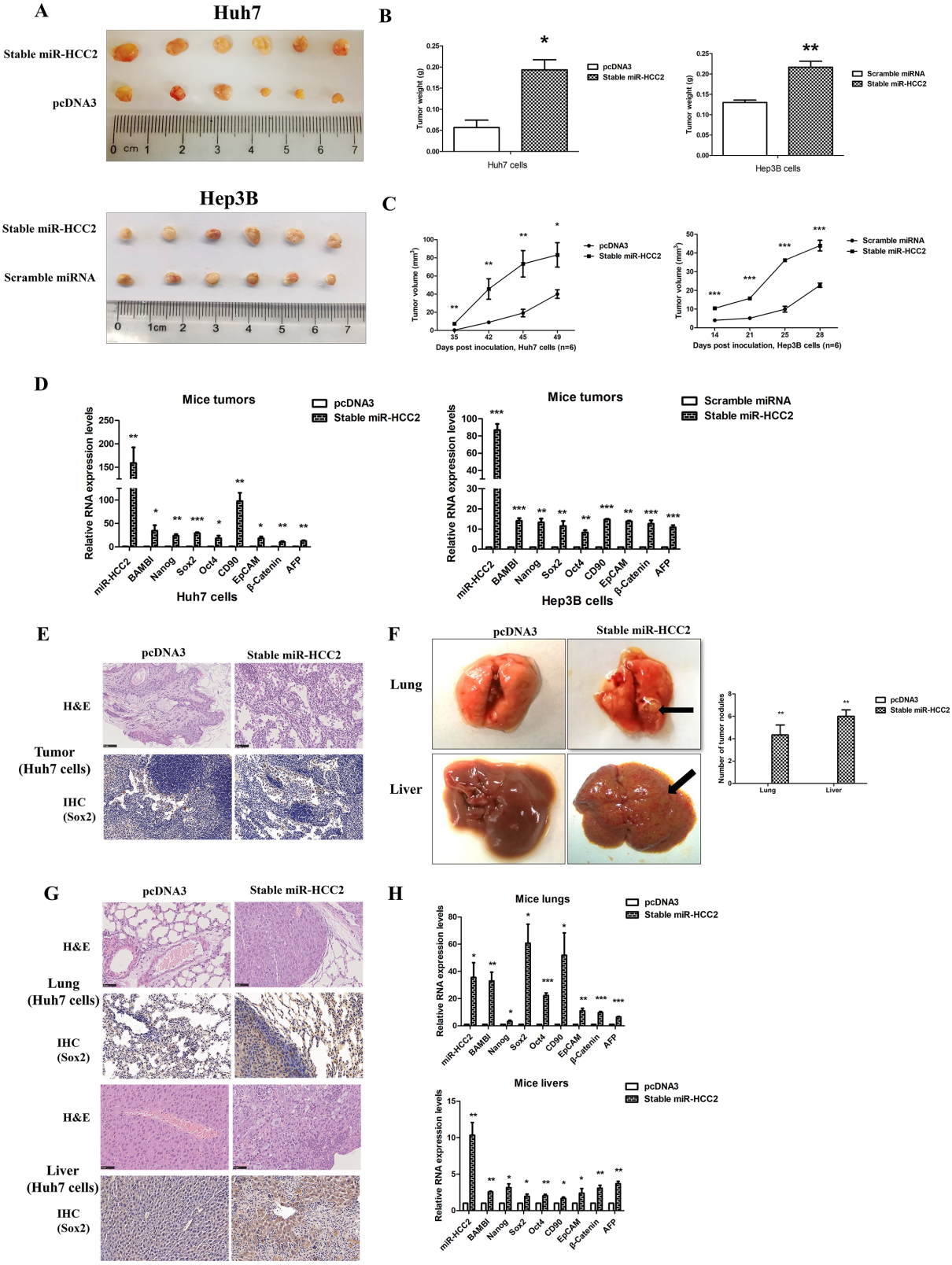

Figure 2. MiR-HCC2 enhanced the proliferation, metastasis and stemness of liver cancer cells *in vivo*. A nude mouse tumor xenograft model was used to evaluate the effects of miR-HCC2 on tumor growth and tumor metastasis *in vivo*. (A) Tumors were isolated from subcutaneously injected mice. The pcDNA3 vector and scrambled miRNA were used as control vector and control miRNA. (B) Tumor weights were quantified after tumors had been isolated from mice. (C) Tumor volumes were assessed after injection. (D) The RNA expression levels of miR-HCC2, BAMBI and stemness markers in mouse tumor nodules. (E) H&E staining and immunohistochemical staining of Sox2 in xenograft tumors from mice that had been injected with Huh7 cells. Scale bar=50 μm. (F) Gross anatomical assessments of lung and liver tissues isolated from intravenously injected mice. Tumor nodules in histological sections of lung and liver tissues were counted. (G) H&E staining and immunohistochemical staining of Sox2 in lungs and livers. Scale bar=50 μm. (H) RNA expression levels of miR-HCC2, BAMBI and stemness markers in lungs and livers. Scale bars=50 μm. All results were compared with corresponding control groups. Data are presented as mean ± standard deviation. *P<0.05, **P<0.01 and ***P<0.001. miR, miRNA; miRNA, micro RNA; Nanog, nanog homeobox; Sox2, sex determining region Y-box 2; Oct4, octamer-binding transcription factor 4; CD90, cluster of differentiation 90; EpCAM, epithelial cellular adhesion molecule; AFP, α-fetoprotein; BAMBI, bone morphogenic protein and activin membrane-bound inhibitor homolog; H&E, hematoxylin and eosin.

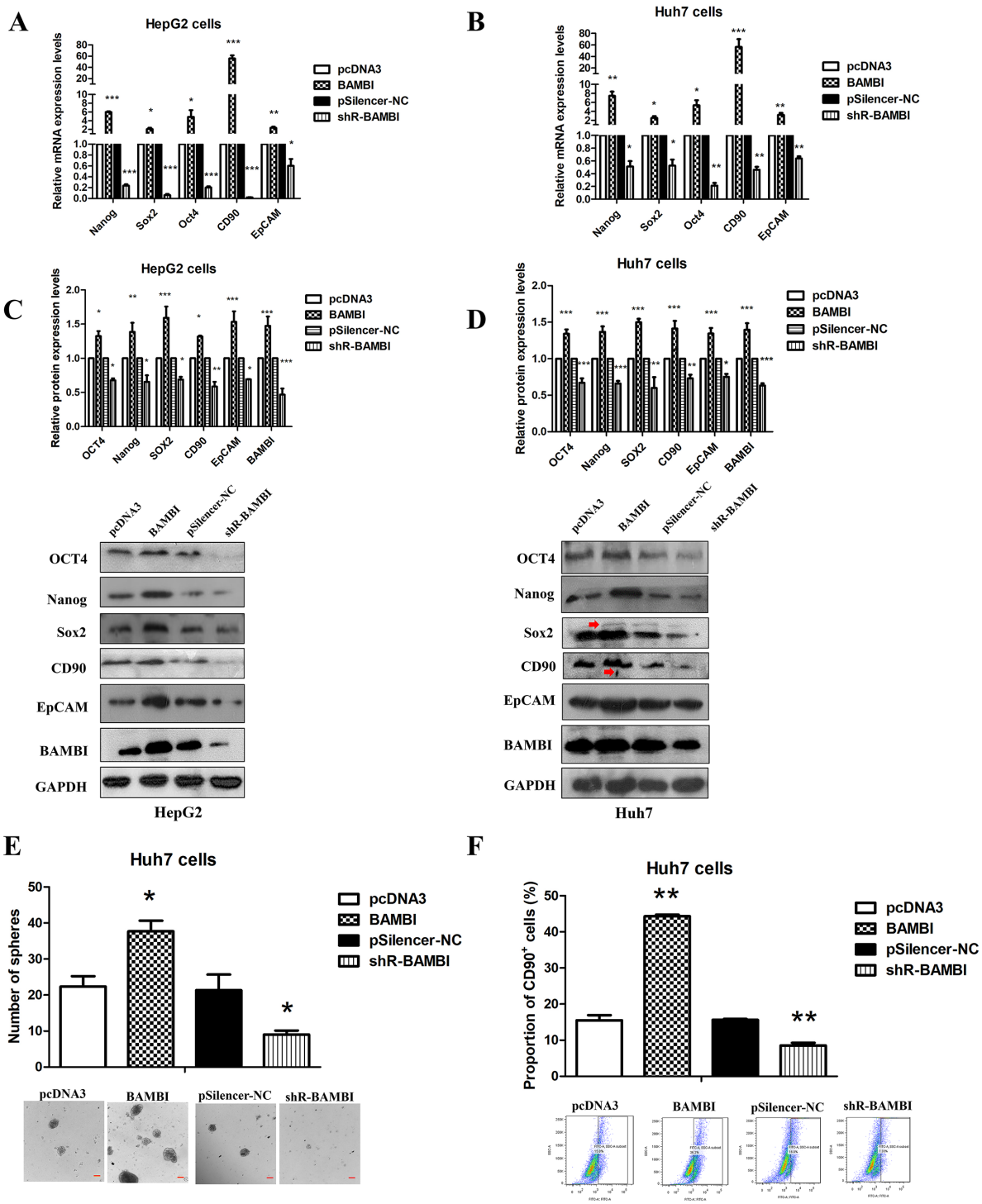

Figure 3. BAMBI promotes stem cell-like properties in human liver cancer cells. The (A and B) mRNA and (C and D) protein expression levels of BAMBI and stemness markers in transfected liver cancer cells were assessed using reverse transcription-quantitative PCR and western blotting assays, respectively. The samples were derived from the same experiment and the blots were processed in parallel. The arrows indicated nonspecific bands. (E) Spheroid formation assays were used to evaluate the impact of BAMBI on tumor sphere-formation ability. Scale bar=100 μm. (F) The proportion of CD90$^+$ cells in liver cancer cells was assessed using flow cytometry analysis. All experiments were performed at least in triplicate. Data are presented as mean ± standard deviation. *P<0.05, **P<0.01 and ***P<0.001 compared with the corresponding control group (BAMBI vs. pcDNA3 and shR-BAMBI vs. pSilencer-NC). Nanog, nanog homeobox; Sox2, sex determining region Y-box 2; Oct4, octamer-binding transcription factor 4; CD90, cluster of differentiation 90; EpCAM, epithelial cellular adhesion molecule; shR, short hairpin RNA; BAMBI, bone morphogenic protein and activin membrane-bound inhibitor homolog; NC, negative control.

that the overexpression of BAMBI significantly increased the β-catenin mRNA and protein expression level and significantly decreased the Axin2 mRNA expression levels, whereas the inhibition of BAMBI significantly decreased the β-catenin mRNA and protein expression level and significantly increased the Axin2 mRNA expression level (Fig. 5A-C). Furthermore, the nuclear expression levels of β-catenin were significantly increased or decreased after BAMBI overexpression or inhibition, respectively, in liver cancer cells; these results suggested that BAMBI promoted nuclear translocation of

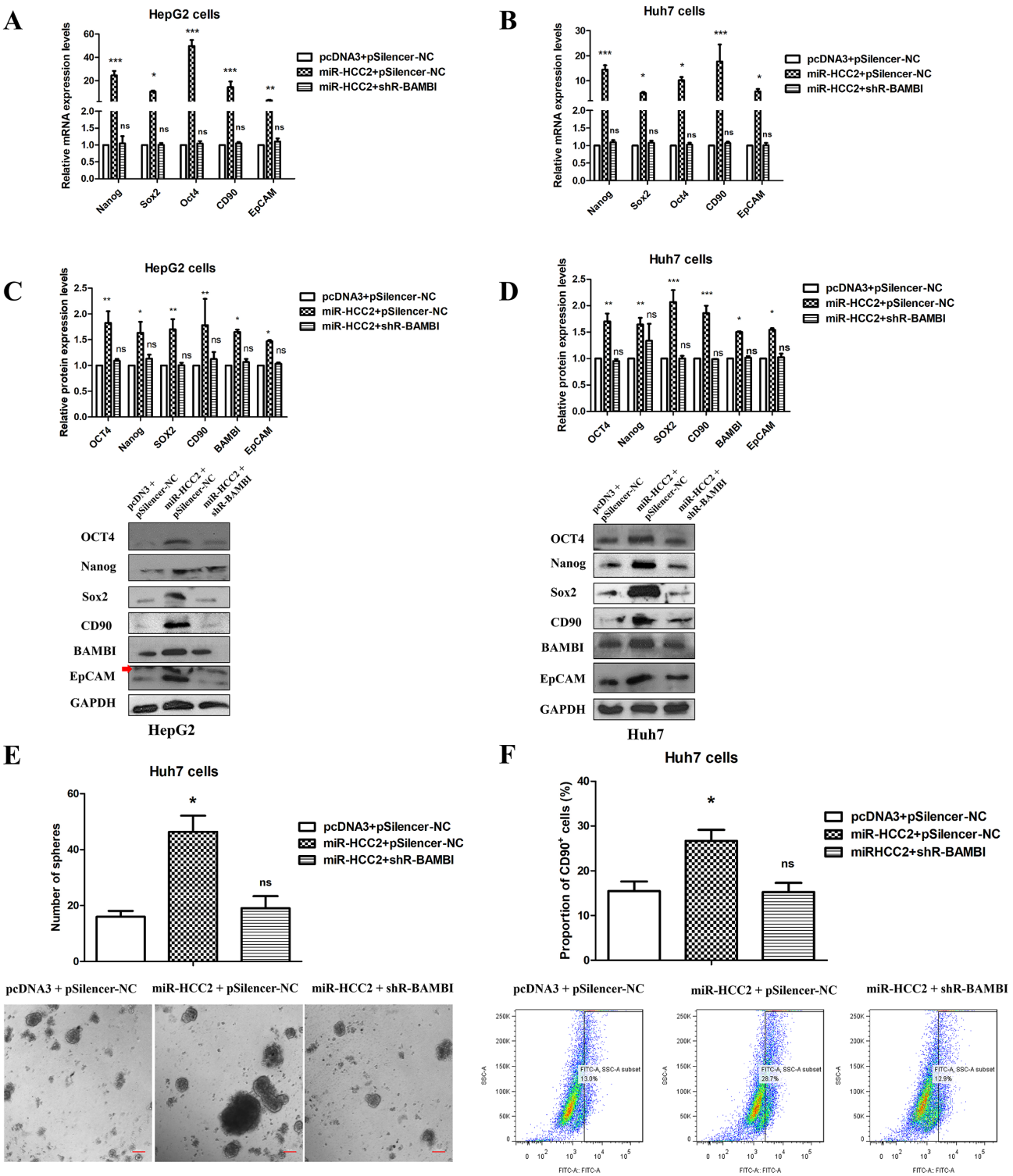

Figure 4. Suppression of BAMBI expression abrogates the effects of miR-HCC2 on stem cell-like properties in human liver cancer cells. The (A and B) mRNA and (C and D) protein expression levels of stemness markers in HepG2 and Huh7 cells were determined after shR-BAMBI transfection in the presence of miR-HCC2. The samples were derived from the same experiment and the blots were processed in parallel. The arrows indicated nonspecific bands. (E) The miR-HCC2-mediated increase in the tumor sphere-forming ability was abrogated by suppression of BAMBI. Scale bar=100 μm. (F) The miR-HCC2-mediated increase in the proportion of $CD90^+$ cells was reduced by suppression of BAMBI. All experiments were performed at least in triplicate. Data are presented as mean ± standard deviation. $^*P<0.05$, $^{**}P<0.01$ and $^{***}P<0.001$ compared with the corresponding control group (miR-HCC2 + pSilencer-NC vs. pcDNA3 + pSilencer-NC and miR-HCC2 + shR-BAMBI vs. pcDNA3 + pSilencer-NC). Nanog, nanog homeobox; Sox2, sex determining region Y-box 2; Oct4, octamer-binding transcription factor 4; CD90, cluster of differentiation 90; EpCAM, epithelial cellular adhesion molecule; shR short hairpin RNA; BAMBI, bone morphogenic protein and activin membrane-bound inhibitor homolog; NC, negative control; miR, microRNA; ns, not significant.

β-catenin (Fig. 5D). Moreover, there was a significant correlation between β-catenin expression and BAMBI expression in mouse tumors (Fig. 5E and F). The aforementioned results indicated that BAMBI could promote the nuclear translocation

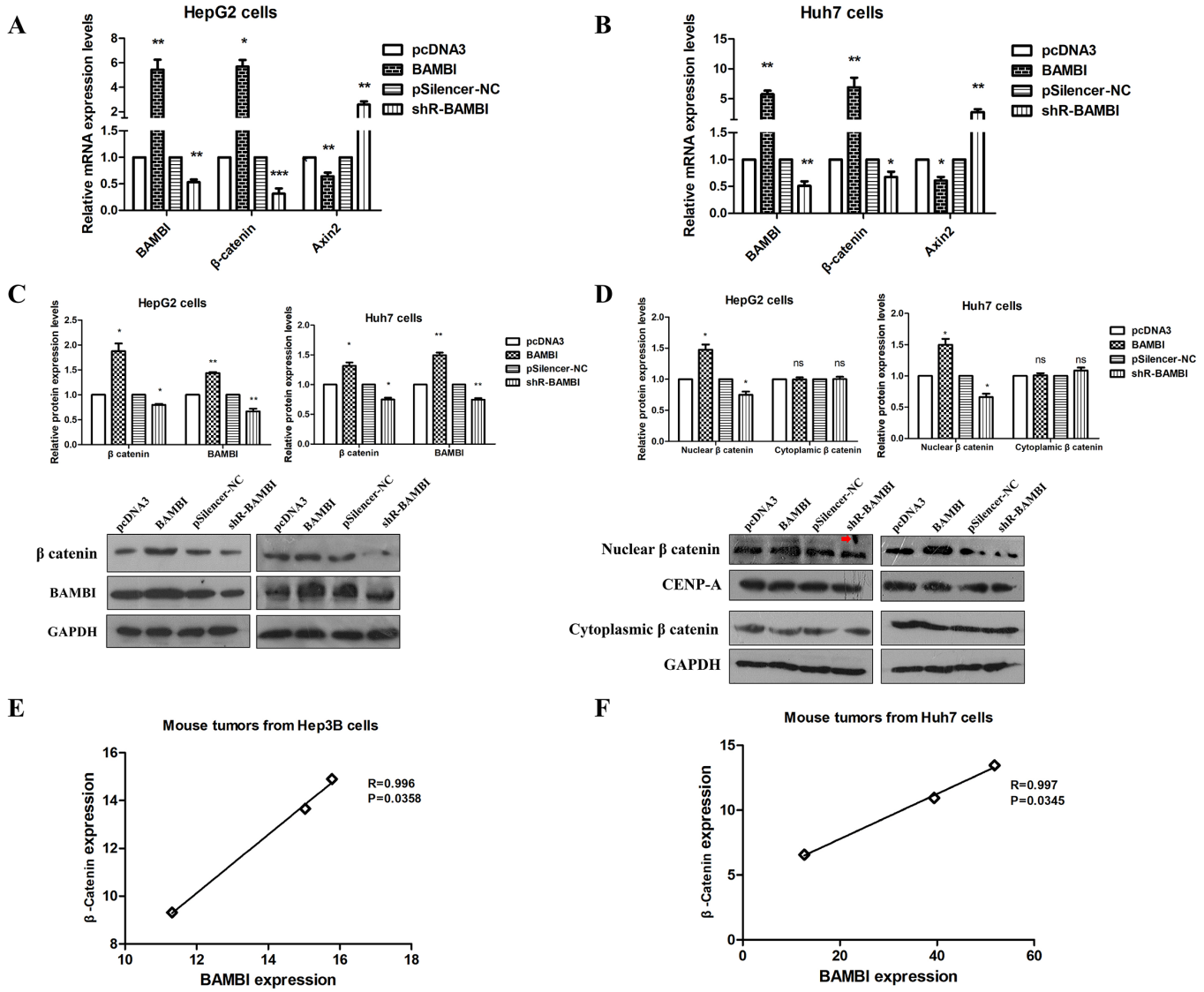

Figure 5. BAMBI promotes nuclear translocation of β-catenin and activates Wnt/β-catenin signaling. Overexpression or knockdown of BAMBI in HepG2 and Huh7 cells significantly increased or decreased the (A and B) mRNA and (C) protein expression levels of β-catenin and decreased or increased the mRNA and expression levels of Axin2. (D) The nuclear translocation of β-catenin was evaluated after overexpression or knockdown of BAMBI. The samples were derived from the same experiment and the blots were processed in parallel. The arrows indicated nonspecific bands. (E and F) Correlation analysis of β-catenin and BAMBI expression levels in mouse tumors. *P<0.05, **P<0.01 and ***P<0.001 compared with the corresponding control group (BAMBI vs. pcDNA3 and shR-BAMBI vs. pSilencer-NC). BAMBI, bone morphogenic protein and activin membrane-bound inhibitor homolog; NC, negative control; shR, short hairpin RNA; Axin2, axis inhibition protein 2; ns, not significant.

of β-catenin, which resulted in activation of the Wnt/β-catenin signaling pathway.

The transcription factor YY1 binds the miR-HCC2 promoter and activates the expression of miR-HCC2. To elucidate the regulatory mechanism underlying the dysregulated expression of miR-HCC2 in liver cancer tissues, bioinformatics analyses were used (Promoter 2.0 and hTFtarget) to predict the miR-HCC2 promoter, along with potential transcription factor binding sites. Several fragments containing putative transcription start sites were separately cloned into pGL3-Basic vectors, including miR-HCC2-promoter1, miR-HCC2-promoter2 and miR-HCC2-promoter3 (Fig. 6A). Luciferase reporter assays demonstrated a significant increase in the luciferase activity of cell transfected with the miR-HCC2-promoter2, which suggested that it contained a functional promoter region (Fig. 6B). Bioinformatic analyses demonstrated that miR-HCC2-promoter2 contained two YY1 binding sites, which were located at 2273-2288 bp and 2883-2 898 bp upstream from pre-miR-HCC2. The ectopic expression or knockdown of YY1 significantly enhanced or decreased the promoter activity of miR-HCC2 in Huh7 cells compared with the controls, which suggested that YY1 could regulate miR-HCC2 expression by enhancing its promoter activity (Figs. 6C and S3). When predicted binding site 1 was mutated, the promoter activity was not affected by the overexpression or inhibition of YY1; however, mutations of predicted binding site 2 demonstrated no effects on YY1 binding. These findings suggested that predicted binding site 1 was responsible for YY1 binding and the subsequent regulation of miR-HCC2 expression (Fig. 6D). Furthermore, miR-HCC2 levels significantly increased or decreased, compared with the control, when

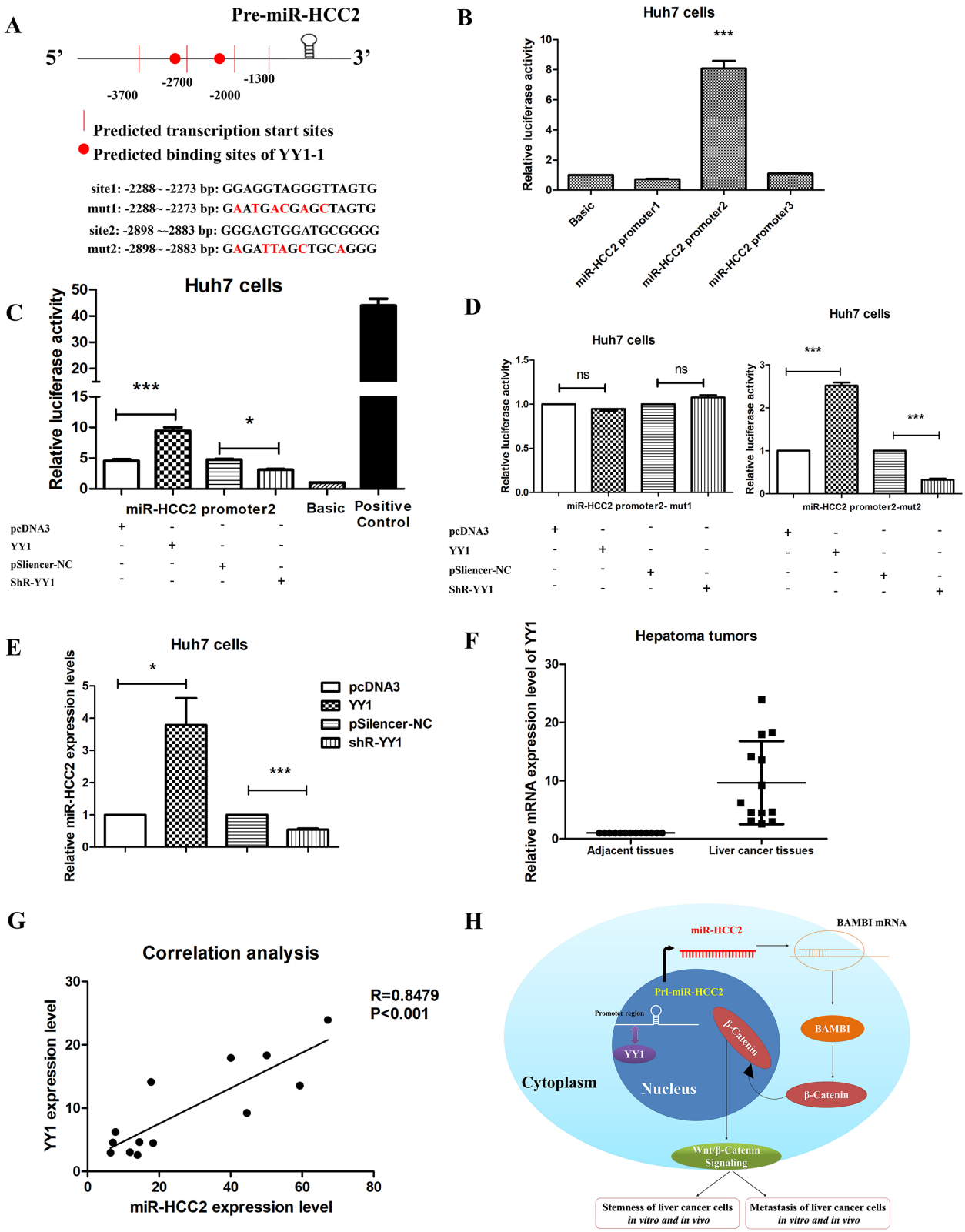

Figure 6. YY1 binds the promoter region and enhances the transcription of miR-HCC2. (A) Promoter 2.0 indicated that predicted transcription start sites were located in the region 1 to 4 kb upstream of pre-miR-HCC2. The predicted YY1 binding sites at nucleotides -2273 to -2288 bp and -2883 to -2898 bp of the miR-HCC2 promoter were identified by hTFtarget. (B) Dual-luciferase assays demonstrated the activities of miR-HCC2 promoter fragment reporters in Huh7 cells. Basic was used as a negative control. ***P<0.001 vs. Basic. (C) Dual-luciferase assays demonstrated the activities of miR-HCC2 promoter fragment reporters upon co-transfection with YY1 or shR-YY1. Basic and pGL3-control were used as negative and positive controls, respectively. *P<0.05 and ***P<0.001 (YY1 vs. pcDNA3 and shR-YY1 vs. pSilencer-NC). (D) Dual-luciferase assays were performed to assess the activities of miR-HCC2 promoter2-mut1 and miR-HCC2 promoter2-mut2 upon transfection with YY1 or shR-YY1. ***P<0.001 (YY1 vs. pcDNA3 and shR-YY1 vs. pSilencer-NC). (E) miR-HCC2 primary transcripts were assessed using RT-qPCR after transfection with YY1 or shR-YY1. *P<0.05 and ***P<0.001 (YY1 vs. pcDNA3 and shR-YY1 vs. pSilencer-NC). (F) YY1 expression levels were assessed using RT-qPCR in 13 pairs of liver cancer tissues. (G) Correlation analysis of YY1 and miR-HCC2 expression levels in liver cancer tissues. All results were compared with corresponding control groups. Data are presented as mean ± standard deviation. (H) Model for role of YY1/miR-HCC2/BAMBI axis in the regulation of stemness in liver cancer cells. miR, microRNA; Basic, pGL3-Basic; ns, not significant; RT-qPCR, reverse transcription-quantitative PCR; BAMBI, bone morphogenic protein and activin membrane-bound inhibitor homolog; Pre, precursor.

YY1 was overexpressed or knocked down in liver cancer cells and correlation analysis demonstrated that YY1 was significantly positively regulated miR-HCC2 in liver cancer tissues (Fig. 6E-G). These results demonstrated that YY1 activated miR-HCC2 transcription by binding to its promoter.

Discussion

Previous studies have reported that CSCs are important for tumor progression in liver cancer because of their high self-renewal capacity, tumorigenicity and chemoresistance (6,7). CSCs have been characterized in solid tumors using stemness markers, including CD90 and certain stemness-related transcriptional factors, such as Nanog, Sox2, EpCAM and Oct4 (8,9,14,38). However, the mechanisms which underlie the regulation of gene expression for those stem cell factors in liver CSCs are unclear. To assess the potential effects of miRNAs on stemness in liver cancer, deep sequencing was used to profile miRNAs isolated from liver cancer tissue samples; which identified certain aberrantly expressed miRNAs. The present study, focused on miR-HCC2, which demonstrated increased expression in liver cancer tissues and has been previously reported to facilitate the growth, migration and invasion of liver cancer cells *in vitro* (32). However, the role of miR-HCC2 in the stemness of liver cancer cells was unclear.

The present study demonstrated that miR-HCC2 was significantly upregulated in liver cancer tissues compared with adjacent non-tumor tissues and that it promoted the stem cell-like properties of liver cancer cells *in vivo* and *in vitro* by targeting BAMBI. Previous studies reported that BAMBI was involved in the regulation of cell proliferation and differentiation in numerous cancers and CSCs through its enhancement of Wnt/β-catenin signaling activity (24,39). For example, BAMBI facilitates an interaction between Frizzled5 and Dishevelled2 that promotes Wnt/β-catenin activity (23). Reduced expression of BAMBI significantly inhibited the nuclear translocation of β-catenin and the transcription of Axin2, two indicators of Wnt/β-catenin activity (40-42). It has been previously reported that activation of the Wnt/β-catenin signaling pathway significantly increased the expression levels of the liver CSC-related molecular markers CD90 and EpCAM, which caused hematopoietic progenitor cells to transform into liver CSCs (43). Therefore, the present study evaluated the effects of BAMBI on the expression and nuclear translocation of β-catenin in liver cancer cells. The results demonstrated that miR-HCC2 influenced the stem cell-like properties of liver cancer cells by targeting BAMBI to promote Wnt/β-catenin signaling. Previous reports indicated that YY1 overexpression contributed to the downregulation of certain tumor suppressor miRNAs, which enhanced NF-κB activation and pro-tumor phenotypes (44,45). However, another study reported that YY1 was a potent inhibitor of c-Myc transforming activity and may have tumor suppressor properties (46). The present study demonstrated that YY1 functioned as an upstream transcription factor that promoted miR-HCC2 expression through direct binding to its promoter region.

The present study also had certain limitations. For instance, the mechanism by which BAMBI promoted nuclear translocation of β-catenin to activate the Wnt/β-catenin signaling pathway in liver cancer cells was not elucidated. YY1 was identified as the upstream transcription factor of miR-HCC2; however, the molecular mechanisms for its high expression and function in liver cancer cells requires further elucidation.

Overall, the present study focused on miR-HCC2, a novel liver cancer-associated miRNA with the second most abundant expression level in liver cancer tissues. Functional analyses demonstrated that miR-HCC2 strongly promoted stemness in liver cancer cells by enhancing the tumor sphere-forming ability, the proportion of $CD90^+$ cells, the expression of stem cell markers, and metastasis *in vitro* and *in vivo* by targeting BAMBI via activation of the Wnt/β-catenin signaling pathway (Fig. 6H). Furthermore, YY1 activated the transcription of pri-miR-HCC2 by binding to the promoter region of miR-HCC2. The results of the present study indicated that YY1-upregulated miR-HCC2 functions as a cancer stemness inducer through the upregulation of BAMBI, which linked the YY1/miR-HCC2/BAMBI axis to the stemness of liver cancer cells. The present study demonstrated the importance of miR-HCC2 as a cancer stemness inducer, thus providing new insights into liver cancer metastasis and recurrence.

Acknowledgements

Not applicable.

Funding

The present study was supported by The National Natural Science Foundation of China (grant nos. 81602410 and 81773002) and The Natural Science Foundation of Tianjin (grant no. 17JCQNJC11300).

Availability of data and materials

The sequence data of miR-HCC2 is available from the NCBI reference sequence database (ID: MH170612.1; https://www.ncbi.nlm.nih.gov/nuccore/MH170612.1/). The datasets used and/or analyzed are available from the corresponding author on reasonable request.

Authors' contributions

HG was responsible for study conception and design. HG, HF and HX were responsible for material preparation, data collection and analysis. HG and HX were responsible for drafting the manuscript. HG and HX confirm the authenticity of all the raw data. All authors read and approved the final manuscript.

Ethics approval and consent to participate

The present study has been reported in accordance with ARRIVE guidelines. All experimental protocols for animals were approved by the Animal Ethics Committee of Tianjin Medical University (approval no. TMULA-201954).

Patient consent for publication

Not applicable.

Competing interests

The authors declare that they have no competing interests.

References

1. El-Serag HB: Hepatocellular carcinoma. N Engl J Med 365: 1118-1127, 2011.
2. Sung H, Ferlay J, Siegel RL, Laversanne M, Soerjomataram I, Jemal A and Bray F: Global cancer statistics 2020: GLOBOCAN estimates of incidence and mortality worldwide for 36 cancers in 185 countries. CA Cancer J Clin 71: 209-249, 2021.
3. Yamashita T and Wang XW: Cancer stem cells in the development of liver cancer. J Clin Invest 123: 1911-1918, 2013.
4. Lee TK, Castilho A, Cheung VC, Tang KH, Ma S and Ng IO: CD24(+) liver tumor-initiating cells drive self-renewal and tumor initiation through STAT3-mediated NANOG regulation. Cell Stem Cell 9: 50-63, 2011.
5. Chan LH, Luk ST and Ma S: Turning hepatic cancer stem cells inside out-a deeper understanding through multiple perspectives. Mol Cells 38: 202-209, 2015.
6. Li XF, Chen C, Xiang DM, Qu L, Sun W, Lu XY, Zhou TF, Chen SZ, Ning BF, Cheng Z, *et al*: Chronic inflammation-elicited liver progenitor cell conversion to liver cancer stem cell with clinical significance. Hepatology 66: 1934-1951, 2017.
7. Sun C, Shui B, Zhao W, Liu H, Li W, Lee JC, Doran R, Lee FK, Sun T, Shen QS, *et al*: Central role of IP3R2-mediated Ca(2+) oscillation in self-renewal of liver cancer stem cells elucidated by high-signal ER sensor. Cell Death Dis 10: 396, 2019.
8. Toraih EA, Fawzy MS, El-Falouji AI, Hamed EO, Nemr NA, Hussein MH and Abd El Fadeal NM: Stemness-related transcriptional factors and homing gene expression profiles in hepatic differentiation and cancer. Mol Med 22: 653-663, 2016.
9. Villasante A, Piazzolla D, Li H, Gomez-Lopez G, Djabali M and Serrano M: Epigenetic regulation of Nanog expression by Ezh2 in pluripotent stem cells. Cell Cycle 10: 1488-1498, 2011.
10. Machida K, Chen CL, Liu JC, Kashiwabara C, Feldman D, French SW, Sher L, Hyeongnam JJ and Tsukamoto H: Cancer stem cells generated by alcohol, diabetes, and hepatitis C virus. J Gastroenterol Hepatol 27 (Suppl 2): S19-S22, 2012.
11. Guo JC, Yang YJ, Zheng JF, Zhang JQ, Guo M, Yang X, Jiang XL, Xiang L, Li Y, Ping H and Zhuo L: Silencing of long noncoding RNA HOXA11-AS inhibits the Wnt signaling pathway via the upregulation of HOXA11 and thereby inhibits the proliferation, invasion, and self-renewal of hepatocellular carcinoma stem cells. Exp Mol Med 51: 1-20, 2019.
12. Moon JH, Kwon S, Jun EK, Kim A, Whang KY, Kim H, Oh S, Yoon BS and You S: Nanog-induced dedifferentiation of p53-deficient mouse astrocytes into brain cancer stem-like cells. Biochem Biophys Res Commun 412: 175-181, 2011.
13. Kumar SM, Liu S, Lu H, Zhang H, Zhang PJ, Gimotty PA, Guerra M, Guo W and Xu X: Acquired cancer stem cell phenotypes through Oct4-mediated dedifferentiation. Oncogene 31: 4898-4911, 2012.
14. Yang ZF, Ho DW, Ng MN, Lau CK, Yu WC, Ngai P, Chu PW, Lam CT, Poon RT and Fan ST: Significance of CD90+ cancer stem cells in human liver cancer. Cancer Cell 13: 153-166, 2008.
15. Croce CM: Causes and consequences of microRNA dysregulation in cancer. Nat Rev Genet 10: 704-714, 2009.
16. Esteller M: Non-coding RNAs in human disease. Nat Rev Genet 12: 861-874, 2011.
17. Kim M, Civin CI and Kingsbury TJ: MicroRNAs as regulators and effectors of hematopoietic transcription factors. Wiley Interdiscip Rev RNA 10: e1537, 2019.
18. Shi DM, Bian XY, Qin CD and Wu WZ: miR-106b-5p promotes stem cell-like properties of hepatocellular carcinoma cells by targeting PTEN via PI3K/Akt pathway. Onco Targets Ther 11: 571-585, 2018.
19. Zheng Z, Liu J, Yang Z, Wu L, Xie H, Jiang C, Lin B, Chen T, Xing C, Liu Z, *et al*: MicroRNA-452 promotes stem-like cells of hepatocellular carcinoma by inhibiting Sox7 involving Wnt/β-catenin signaling pathway. Oncotarget 7: 28000-28012, 2016.
20. Onichtchouk D, Chen YG, Dosch R, Gawantka V, Delius H, Massagué J and Niehrs C: Silencing of TGF-beta signalling by the pseudoreceptor BAMBI. Nature 401: 480-485, 1999.
21. Yan X, Lin Z, Chen F, Zhao X, Chen H, Ning Y and Chen YG: Human BAMBI cooperates with Smad7 to inhibit transforming growth factor-beta signaling. J Biol Chem 284: 30097-30104, 2009.
22. Mai Y, Zhang Z, Yang H, Dong P, Chu G, Yang G and Sun S: BMP and activin membrane-bound inhibitor (BAMBI) inhibits the adipogenesis of porcine preadipocytes through Wnt/β-catenin signaling pathway. Biochem Cell Biol 92: 172-182, 2014.
23. Lin Z, Gao C, Ning Y, He X, Wu W and Chen YG: The pseudoreceptor BMP and activin membrane-bound inhibitor positively modulates Wnt/beta-catenin signaling. J Biol Chem 283: 33053-33058, 2008.
24. Zhang Q, Shi XE, Song C, Sun S, Yang G and Li X: BAMBI Promotes C2C12 myogenic differentiation by enhancing Wnt/β-Catenin signaling. Int J Mol Sci 16: 17734-17745, 2015.
25. Liu K, Song X, Ma H, Liu L, Wen X, Yu J, Wang L and Hu S: Knockdown of BAMBI inhibits β-catenin and transforming growth factor β to suppress metastasis of gastric cancer cells. Mol Med Rep 10: 874-880, 2014.
26. Tang T, Guo C, Xia T, Zhang R, Zen K, Pan Y and Jin L: LncCCAT1 promotes breast cancer stem cell function through activating WNT/β-catenin signaling. Theranostics 9: 7384-7402, 2019.
27. Hoffmeyer K, Raggioli A, Rudloff S, Anton R, Hierholzer A, Del Valle I, Hein K, Vogt R and Kemler R: Wnt/β-catenin signaling regulates telomerase in stem cells and cancer cells. Science 336: 1549-1554, 2012.
28. Lu J, Wei JH, Feng ZH, Chen ZH, Wang YQ, Huang Y, Fang Y, Liang YP, Cen JJ, Pan YH, *et al*: miR-106b-5p promotes renal cell carcinoma aggressiveness and stem-cell-like phenotype by activating Wnt/β-catenin signalling. Oncotarget 8: 21461-21471, 2017.
29. Bentley DR: Whole-genome re-sequencing. Curr Opin Genet Dev 16: 545-552, 2006.
30. Livak KJ and Schmittgen TD: Analysis of relative gene expression data using real-time quantitative PCR and the 2(-Delta Delta C(T)) method. Methods 25: 402-408, 2001.
31. Edwards M, Wong SC, Chotpadiwetkul R, Smirlis D, Phillips IR and Shephard EA: Transfection of primary cultures of rat hepatocytes. Methods Mol Biol 320: 273-282, 2006.
32. Yi J, Fan Y, Zhang L, Wang H, Mu T, Xie H, Gao H, Liu M, Li S and Tang H: MiR-HCC2 Up-regulates BAMBI and ELMO1 expression to facilitate the proliferation and EMT of hepatocellular carcinoma cells. J Cancer 10: 3407-3419, 2019.
33. Chen T, Dai X, Dai J, Ding C, Zhang Z, Lin Z, Hu J, Lu M, Wang Z, Qi Y, *et al*: AFP promotes HCC progression by suppressing the HuR-mediated Fas/FADD apoptotic pathway. Cell Death Dis 11: 822, 2020.
34. Saliminejad K, Khorram Khorshid HR, Soleymani Fard S and Ghaffari SH: An overview of microRNAs: Biology, functions, therapeutics, and analysis methods. J Cell Physiol 234: 5451-5465, 2019.
35. Mani SK, Zhang H, Diab A, Pascuzzi PE, Lefrançois L, Fares N, Bancel B, Merle P and Andrisani O: EpCAM-regulated intramembrane proteolysis induces a cancer stem cell-like gene signature in hepatitis B virus-infected hepatocytes. J Hepatol 65: 888-898, 2016.
36. Nusse R: Wnt signaling and stem cell control. Cell Res 18: 523-527, 2008.
37. de Sousa E Melo F and Vermeulen L: Wnt signaling in cancer stem cell biology. Cancers (Basel) 8: 60, 2016.
38. Shaikh MV, Kala M and Nivsarkar M: CD90 a potential cancer stem cell marker and a therapeutic target. Cancer Biomark 16: 301-307, 2016.
39. Shangguan L, Ti X, Krause U, Hai B, Zhao Y, Yang Z and Liu F: Inhibition of TGF-β/Smad signaling by BAMBI blocks differentiation of human mesenchymal stem cells to carcinoma-associated fibroblasts and abolishes their protumor effects. Stem Cells 30: 2810-2819, 2012.
40. Jho EH, Zhang T, Domon C, Joo CK, Freund JN and Costantini F: Wnt/beta-catenin/Tcf signaling induces the transcription of Axin2, a negative regulator of the signaling pathway. Mol Cell Biol 22: 1172-1183, 2002.
41. Leung JY, Kolligs FT, Wu R, Zhai Y, Kuick R, Hanash S, Cho KR and Fearon ER: Activation of AXIN2 expression by beta-catenin-T cell factor. A feedback repressor pathway regulating Wnt signaling. J Biol Chem 277: 21657-21665, 2002.

42. Zhang L, Shi S, Zhang J, Zhou F and ten Dijke P: Wnt/β-catenin signaling changes C2C12 myoblast proliferation and differentiation by inducing Id3 expression. Biochem Biophys Res Commun 419: 83-88, 2012.
43. Zhu K, Li J, Sun J, Sun J, Guo Y, Tian H, Li L, Zhang C, Shi M, Kong G and Li Z: Ring1 promotes the transformation of hepatic progenitor cells into cancer stem cells through the Wnt/β-catenin signaling pathway. J Cell Biochem 121: 3941-3951, 2020.
44. Wang H, Garzon R, Sun H, Ladner KJ, Singh R, Dahlman J, Cheng A, Hall BM, Qualman SJ, Chandler DS, *et al*: NF-kappaB-YY1-miR-29 regulatory circuitry in skeletal myogenesis and rhabdomyosarcoma. Cancer Cell 14: 369-381, 2008.
45. Tsang DP, Wu WK, Kang W, Lee YY, Wu F, Yu Z, Xiong L, Chan AW, Tong JH, Yang W, *et al*: Yin Yang 1-mediated epigenetic silencing of tumour-suppressive microRNAs activates nuclear factor-κB in hepatocellular carcinoma. J Pathol 238: 651-664, 2016.
46. Austen M, Cerni C, Luscher-Firzlaff JM and Luscher B: YY1 can inhibit c-Myc function through a mechanism requiring DNA binding of YY1 but neither its transactivation domain nor direct interaction with c-Myc. Oncogene 17: 511-520, 1998.